IMAGING ERROR FROM MISLOCATION OF SURFACE SENSORS: SENSITIVITY, DETECTION, AND ESTIMATE CORRECTION, WITH APPLICATION TO EIT

Saeed Babaeizadeh, Dana H. Brooks

Northeastern University
Department of Electrical and Computer Engineering
Boston, MA, USA

ABSTRACT

The accuracy of the inverse solutions obtained by imaging modalities which use surface measurements can be significantly reduced by even small modeling errors. One important type of modeling error is inaccuracy in locating the sensors. In this paper, we first report on the sensitivity to sensor mislocation of a known-geometry inverse solution both through simulation and by calculating the Cramér-Rao Lower Bound on the estimate variance. We then introduce a method based on a likelihood ratio hypothesis test to use the statistical behavior of the residuals to identify potential sensor mislocation. Upon detection of sensor location error, we then propose an approach, based on Principal Component Analysis of the residuals, to reduce the sensitivity of the reconstruction algorithm to this kind of modeling error. We show the simulation results using a method, introduced in our previous work, for Electrical Impedance Tomography based on Boundary Element Methods.

1. INTRODUCTION

Many imaging modalities estimate an unknown value inside a volume from measurements on its surface. Typical examples are Electrical Impedance Tomography (EIT), which estimates the conductivity map inside a volume from electrical measurements on its surface, and Diffuse Optical Tomography (DOT) in which optical properties are estimated using optical surface sensors. These imaging modalities are in general badly posed, and thus are sensitive to even small modeling errors. In modalities which depend on spatially-localized surface measurement sensors, inaccuracy in locating those sensors is an important type of modeling error. Indeed, for EIT, recent reports show that accurate electrode position is a critical component to obtain good static conductivity maps [1, 2]. In this work, we concentrate on EIT as our application of interest, and thus the details of our forward modeling and inverse solution are EIT-specific, but the problem, the approach, and the proposed improvement are more widely applicable.

In our approach to EIT, in which we are interested in imaging inside the torso, head, or other region of the body, we stabilize the ill-posedness by assuming that the value of interest is piecewise constant inside the volume, with a relatively small number of distinct regions, *e.g.,* various internal organs in the torso, and that the region boundaries are known, for example from prior anatomical imaging. In this technique, if the geometric model is accurate enough, the forward problem can be solved to within the precision of the measurement system, which makes it possible to obtain a reliable image [3]. The effects of inaccuracy in locating the surface sensors have been studied by many researchers; for example see [1, 4]. Since there are no common parameters between these papers, the results of them are difficult to compare with each other.

Based on the known-geometry and piecewise-constant conductivity assumptions mentioned above, in [5, 6, 7] we have introduced two EIT algorithms, one based on the Boundary Element Method (BEM) and the other on the Finite Element Method (FEM). In this paper, we first briefly report the results of our study on the sensitivity of those inverse EIT techniques to electrode mislocation via calculation of the Cramér-Rao Lower Bound (CRLB) on the estimate variance. We then present a method to use the statistical behavior of the residuals to identify potential sensor mislocation, based on a likelihood ratio hypothesis test. Upon detection of sensor location error, we propose an approach, based on Principal Component Analysis (PCA) of the residuals, to reduce the sensitivity of the reconstruction algorithm to this kind of modeling error. We emphasize that although we show the simulation results only for EIT, the same methods and discussion are valid for other imaging modalities which use surface measurements.

2. SENSITIVITY TO SENSOR LOCATION ERROR

Fig. 1 shows the geometry which we used for our modeling and simulations. To test the sensitivity of our known-geometry BEM-based inverse EIT solution to electrode misplacement, we computed a forward model using the geometry shown in Fig. 1, but simulated the measurements using the same model but with the electrodes misplaced. No other noise was added to the measurements. We have both run Monte-Carlo testing and calculated the CRLB for a variety of measurement protocols and two different imaging types. The CLRB calculation is based on the analytical expression for the Jacobian, which we describe for our BEM and FEM forward models in [5, 6]. The CRLB results, which agree with the Monte-Carlo simulations, show that the background conductivity estimated fairly stably with one electrode mislocated by as much as 20% of its size if one uses an appropriate method to inject current and measure voltage. (In particular it is key to measure voltage on the electrodes which are injecting current.) However, the conductivity of the inhomogeneity is much more sensitive, with a variance considerably larger than the value of the conductivity itself with 20% mislocation error of only one electrode.

The work of the authors was supported in part by the National Institutes of Health, National Center for Research Resources, grant number 1-P41-RR12553-3, and in part by CenSSIS, the Center for Subsurface Sensing and Imaging Systems, under the Engineering Research Centers Program of the National Science Foundation, award number EEC-9986821.

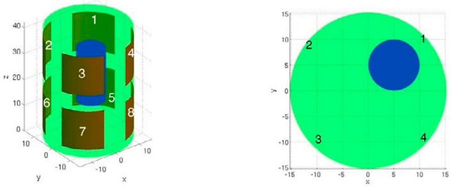

(a) Side view. (b) Top view.

Fig. 1. Computational geometry showing the test tank, internal inhomogeneity, and eight surface electrodes.

3. DETECTING THE SENSOR MISLOCATION

In this section we apply a detection procedure to test for the presence of mis-located sensors. If there is no error in the sensor positions, and the forward model is reasonably accurate, we expect the difference between the measurement and the model prediction, *i.e.*, the residual, to be merely due to measurement noise, and hence spatially uncorrelated. In this section we describe a procedure to apply an appropriate statistical test from the multivariate statistical literature to test whether the residuals are in fact uncorrelated. The procedure is based on making multiple measurements; in EIT one does this by necessity either by using different combination of current injection electrodes or by using a set of different weights on the injection electrodes to create a sequence of spatial “current injection patterns”.

Let $X_1, X_2, \ldots, X_N$ denote the residual vectors corresponding to N different measurements. Each vector has L elements, where L is the total number of sensors. Let us assume these residuals are independent $N_L(\mu, \Sigma)$ random vectors. Now if these residuals are only due to the measurement noise (and hence spatially uncorrelated), the spatial covariance, denoted by Σ, will have the structure of an identity matrix. Therefore, testing the hypothesis that there is electrode misplacement in the model is equivalent to testing the null hypothesis $H_0 : \Sigma = \lambda I_L$ against the alternative $H_1 : \Sigma \neq \lambda I_L$, where λ is unspecified. This null hypothesis H_0 in the statistics community is called the *hypothesis of sphericity*, because when it is true, the contours of equal density in the normal distribution are hyperspheres [8].

We use a Neyman-Pearson approach in which we fix the size of the test α, *i.e.* , the probability of rejecting H_0 when in fact it is true (Type I error), and then find a test which minimizes the type II error, mistakenly accepting H_0. This leads to a likelihood ratio test. For testing sphericity, it is shown in [8] that the likelihood ratio test of size α of $H_0 : \Sigma = \lambda I_L$, where λ is unspecified, rejects H_0 if

$$V_0 \equiv \frac{\det S}{\left(\frac{1}{L}\operatorname{tr} S\right)^L} \leq k_\alpha, \tag{1}$$

where $S = \frac{1}{N-1}\sum_{i=1}^{N}\left(X_i - \bar{X}\right)\left(X_i - \bar{X}\right)^T$, and k_α is chosen so that the size of test is α.

Determining the threshold k_α and calculating the power of the test requires the distribution of V_0, commonly called the *ellipticity statistic* [8]. Some distributional results have been obtained in [8]; the details are beyond the scope of this paper. Except in some special cases, the exact distributions are extremely complicated, and so asymptotic distributions are often used. Here, we use the asymptotic distribution of the likelihood ratio statistic first given explicitly by Anderson [9]. Using this distribution, we can compute a p-value:

$$p\text{-value} = P\left(\chi_f^2 = x\right) + \frac{\gamma}{M^2}\left[P\left(\chi_{f+4}^2 = x\right) - P\left(\chi_f^2 = x\right)\right], \tag{2}$$

where

$$\begin{aligned} \gamma &= \frac{(L+1)(L-1)(L+2)(2L^3+6L^2+3L+2)}{288L^2}, \\ M &= (N-1) - \frac{2L^2+L+2}{6L}, \\ x &= -M\log V_0, \qquad f = \frac{L(L+1)}{2} - 1, \end{aligned}$$

and $P\left(\chi_f^2 = x\right)$ is the χ^2 cumulative distribution function (cdf) with f degrees of freedom at x. After computing the p-value, we decide the sphericity test as:

$$\begin{cases} p\text{-value} \leq \alpha \Rightarrow \text{reject } H_0 \Rightarrow \text{sphericity not reasonable} \\ p\text{-value} > \alpha \Rightarrow \text{accept } H_0 \Rightarrow \text{sphericity reasonable.} \end{cases}$$

If we reject H_0 we believe that the electrodes are misplaced. In the next section we propose a technique to reduce our sensitivity to this mislocation when we detect it.

4. SENSITIVITY REDUCTION

We now propose an approach based on Principal Component Analysis (PCA) to reduce the sensitivity of the inverse solution to the sensor misplacement, and hence to improve the reconstruction results, if sensor mislocation is detected by the procedure described in the preceeding section.

If the null hypothesis of Sec. 3 is rejected, it is still possible that the $L-1$ smallest eigenvalues are equal. If this is true, and if their common value (or rather an estimate of it) is small compared to the largest (estimated) eigenvalue, then most of the variation in the sample is explained by the first principal component. In that case we can filter out the effects of the sensor location error by projecting the entire problem onto the subspace defined by the remaining $L-1$ eigenvectors. Even if a test for statistical equality among the $L-1$ smallest eigenvalues is rejected, we can test whether the $L-2$ smallest eigenvalues of Σ are statistically equal, and so on. In practice then, we test sequentially the null hypotheses

$$H_k : \lambda_{k+1} = \cdots = \lambda_L, \tag{3}$$

for $k = 0, 1, \cdots, L-2$, where $\lambda_1 \geq \cdots \geq \lambda_L > 0$ are the eigenvalues of Σ. We saw in Sec. 3 that the likelihood ratio test of $H_0 : \lambda_1 = \cdots = \lambda_L$ is based on the ellipticity statistic V_0 in (1). The likelihood ratio statistic for testing the null hypothesis (3) is $V_k^{N/2}$, where

$$V_k \equiv \frac{\prod_{i=k+1}^{L} s_i}{\left(\frac{1}{L-k}\sum_{i=k+1}^{L} s_i\right)^{L-k}}. \tag{4}$$

The proof can be found in [8].

Going through the details of deriving the asymptotic distribution of the statistic V_k when the null hypothesis H_k is true, once again, is out of the scope of this paper; details are in [8]. If N is large, it is shown there that an approximate test of size α of the null hypothesis H_k is to reject H_k if

$$P_k > c\left(\alpha;\ \frac{(q+2)(q-1)}{2}\right) \tag{5}$$

where

$$P_k = -\left[N - k - \frac{2q^2+q+2}{6q} + \sum_{i=1}^{k}\frac{\bar{s}_q^2}{(s_i-\bar{s}_q)^2}\right]\log V_k,$$

$$q = L - k, \qquad \bar{s}_q = \frac{1}{q}\sum_{i=k+1}^{L} s_i,$$

and $c(\alpha;\ r)$ is the upper $100\alpha\%$ point of the χ_r^2 distribution.

Our algorithm, then, when it detects electrode error by rejecting H_0, sequentially tests the null hypotheses H_k, $k = 1, \cdots, L-2$, to find the $L-k$ smallest equal eigenvalues of Σ. We assume these equal eigenvalues correspond to the spatially white Gaussian measurement noise, and thus that the corresponding principal component eigenvectors span the space of the measurement noise and that the remaining eigenvectors correspond to the error in the knowledge of the sensor locations. Therefore, we may hope to reduce the effects of the sensor mislocation on the residuals by projecting onto the measurement noise space. In order to apply this idea, we run our inverse solution a second time, initializing the unknowns at the values retrieved by the first run of the inverse solution, and projecting the residuals to the measurement noise space.

5. RESULTS

We used our BEM-based known-geometry inverse EIT method [5] and the geometry shown in Fig. 1 for our simulations. We randomly moved all eight electrodes, moving each electrode according to a uniform random variate up to 5% of its size to either the left or right. We defined the average movement of the electrodes as the ratio of the sum of the absolute misplacement of all the electrodes to the total number of electrodes. Due to the discretized specifications of the tank boundary mesh, this average movement is a number in $\{0 : 0.625 : 5\}$ (in MATLAB notation). We repeated the random trials enough times to ensure that we have all of the values in this sequence represented in our data set at least 7 times, then averaged over the results corresponding to the same average percent movement of the electrodes. (Note this means that the number of trials per any particular averaged movement is thus a variable.) In the results presented here we had between 7 and 12 trials for each value of the average; the resulting number of trials for each case is reported in the last column of Table 1. After moving the electrodes, we simulated the application of current patterns which would be optimal for the homogeneous cylindrical tank and calculated the voltage on the electrodes. We then added spatially uncorrelated Gaussian noise at a specified SNR to these voltages to simulate the measurements for a system in which both sources of noise exist: electrode mislocation and measurement noise. Using eight electrodes we can apply only seven linearly independent current patterns; to reduce the variance of our estimate of S, and thus the accuracy of the sphericity test, we applied the same set of seven current patterns several times, with different measurement noise. We used the noisy voltages from the repeated applications to estimate S but only used the measurements from the first set for our inverse solution, that is to retrieve the unknown conductivities.

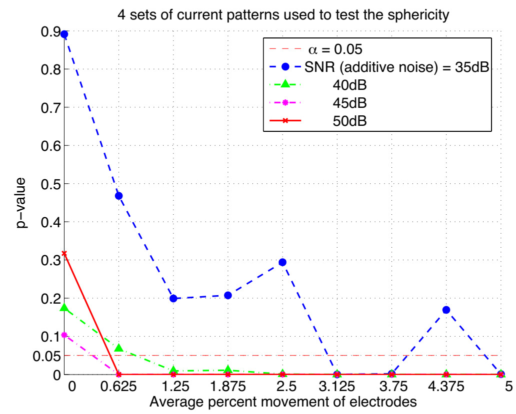

Fig. 2. p-values as a function of the average percent movement of the eight electrodes, for different signal to (additive) noise ratios; four repetitions of the set of optimal current patterns was used to compute the p-values. True values: $\sigma_1 = 1$ and $\sigma_2 = 4$.

We note that this repeated application of the currents is not a problem in practice; once the measurement setup is in place it is easy and fast to apply the current patterns repeatedly.

Fig. 2 shows the p-values resulting from the sphericity test, as a function of the average percent movement of the eight electrodes, for different signal to (measurement) noise ratios. We used four repetitions of the seven sets of current patterns to compute the p-values in order to decide if the electrodes were misplaced or not. Whenever the p-value is less than $\alpha = 0.05$ (shown as a dashed line on Fig. 2), the algorithm reports that the electrodes are misplaced. We observe that for high SNR the algorithm detected the electrode misplacement, even as small as 0.625%, with good accuracy (small p-value). When the SNR was low (35dB), the algorithm did not perform well. Other than the 35dB SNR case, the only mistake the algorithm made, *i.e.* wrongly accepting the hypothesis of "no electrode mislocation" (a type II error), was when SNR was 40dB and the average percent movement of the electrodes was 0.625%.

One may expect to improve the performance by using more current patterns, and hence more measurements. To test this idea, we used different numbers of repeatitions of the sets of current patterns at an SNR of 40dB; results are shown in Fig. 3. As expected, the algorithm performed better when using more current patterns. Using more than six sets of current patterns, the algorithm detected 0.625% average movement of the electrodes. Even for 35 dB (results not shown here to save space), by using nine extra sets of current patterns the algorithm was able to detect the electrode mislocation when the average percent movement of the electrodes was 1% or more.

To test the technique we proposed to reduce the sensitivity of the reconstruction to the sensor mislocation, we used the same data and geometry described before. Table 1 shows the results for the case where SNR due to the additive spatially white Gaussian noise is 40dB. In this table, we report the reconstruction errors for both σ_1 and σ_2 after the first run of the inverse solution, $\Delta\sigma_1$ and $\Delta\sigma_2$, as well as the reconstruction error for σ_2 after the second run of the inverse solution, $\Delta\sigma_2'$. For the second run of the inverse solution, since we have observed from CLRB and Monte-Carlo experiments that the background conductivity, even with sensor misplacement

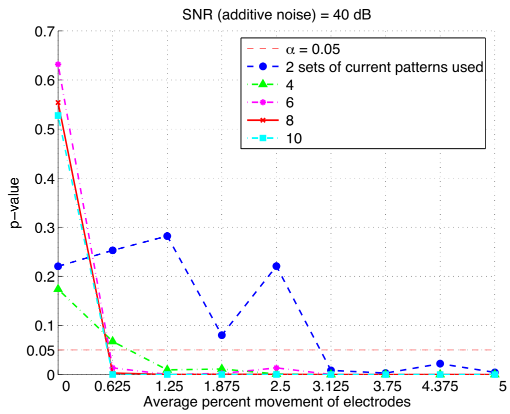

Fig. 3. p-values as a function of the average percent movement of the eight electrodes, using different numbers of repetitions of optimal current patterns, with SNR=40dB.

Table 1. Percent error in retrieved conductivities after the first and second runs of the inverse solution for the model shown in Fig. 1 as a function of the average percent movement of the eight electrodes. SNR due to the additive spatially white Gaussian noise is 40dB

SNR = 40dB				
Average Elecs Movement (%)	1^{st} Run		2^{nd} Run	No. of Trials
	$\Delta\sigma_1(\%)$	$\Delta\sigma_2(\%)$	$\Delta\sigma_2'(\%)$	
0.625	0.1	15.7	21.4	9
1.250	0.2	16.3	19.1	12
1.875	0.1	17.6	11.3	10
2.500	0.2	21.7	10.2	9
3.125	0.2	23.1	15.9	8
3.750	0.1	27.6	17.2	7
4.375	0.1	26.9	21.4	10
5.000	0.2	26.1	18.7	8

in the model, can be retrieved accurately, we fixed σ_1 at the value found in the first run of the inverse solution to allow our non-linear inverse solution to converge more rapidly. In these simulations, in which eight electrodes were used, the algorithm projected the residuals to the space spanned by the seven principal component coefficient vectors corresponding to the seven smallest eigenvalues of the spatial covariance matrix, as suggested by the nested sphericity tests described above.

We observe that we have been able to reduce the reconstruction error for σ_2 when the average movement of the electrodes is 1.5% or more. For example, we could reduce this error by more than 10% when the electrodes had been misplaced by 2.5% on average. It is also interesting to note that when the electrodes mislocation is small, although the algorithm is able to detect it, ignoring the largest principal component of the residuals increases the reconstruction error. One reason may be that in this case, by ignoring that principal component, we lose more useful information than we gain by suppressing the noise incurred from the electrode misplacement. We note that using the p-value for each test, we can decide if the electrodes misplacement detected by the algorithm is small, and thus if there is no need to run the inverse solution for the second time.

6. CONCLUSIONS AND DISCUSSION

Even a small error in the knowledge of the sensor positions may produce a large error in retrieving the unknown values using imaging modalities which use surface measurements, as confirmed by both CLRB results and Monte-Carlo studies in the case of known-geometry EIT. To detect potential sensor mislocation, having the geometrical model of the object, we proposed a method based on statistical hypothesis testing. If misplacement of the sensors is detected, we can reduce the effect of this sensor mislocation in an inverse solution for the conductivities using the PCA-based technique we proposed in this paper.

The methods proposed require that the experimenter make extra measurements while collecting the data; however this can easily and rapidly be done when the experimental setup is ready.

We implemented the algorithms in MATLAB with some help from the Statistic Toolbox. Testing the sphericity can be done rapidly; if sensor mislocation is detected, applying the PCA-based technique requires a second run of our iterative inverse solution, which increases the total computational burden of the reconstruction process.

Studying other invariant test statistics which can be used for the sphericity test, and improving the sensitivity reduction technique, are subjects of on-going work.

7. REFERENCES

[1] V. Kolehmainen, M. Vauhkonen, P. A. Karjalainen, and J. P. Kaipio, "Assessment of errors in static electrical impedance tomography with adjacent and trigonometric current patterns," *Physiological Measurements*, vol. 18, no. 4, Nov. 1997.

[2] Robert P. Patterson, Jie Zhang, Lynne I. Mason, and Michael Jerosch-Herold, "Variability in the cardiac EIT image as a function of electrode position, lung volume and body position," *Physiological Measurements*, vol. 22, no. 1, 2001.

[3] Kuo-Sheng Cheng, David Isaacson, J. C. Newell, and D. G. Gisser, "Electrode models for electric current computed tomography," *IEEE Transactions on Biomedical Engineering*, vol. 36, no. 9, September 1989.

[4] D. C. Barber and B. H. Brown, "Errors in reconstruction of resistivity images using a linear reconstruction technique.," *Clin. Phys. Physiol. Meas.*, vol. 9, pp. A101–A104, 1988.

[5] Saeed Babaeizadeh, Dana H. Brooks, and David Isaacson, "3-D electrical impedance tomography for piecewise constant domains with known internal boundaries," submitted to IEEE Transactions on Biomedical Engineering, under review, 2005.

[6] Saeed Babaeizadeh, Dana H. Brooks, and David Isaacson, "Electrical impedance tomography using a 3-D boundary element inverse solution," in *Thirty-Eight Asilomar Conference on Signals, Systems & Computers*, Nov. 2004, pp. 1595–1599.

[7] Saeed Babaeizadeh, Dana H. Brooks, and David Isaacson, "A 3-D boundary element solution to the forward problem of electrical impedance tomography," in *Proceedings of the 26th Annual International Conference of the IEEE EMBS*, San Francisco, CA, USA, September 2004, pp. 960–963.

[8] Robb J. Muirhead, *Aspects Of Multivariate Statistical Theory*, John Wiley and Sons, Ltd, May 1982.

[9] T. W. Anderson, *An Introduction to Multivariate Statistical Analysis*, chapter 10.7.4, 1st. John Wiley and Sons, Ltd, 1958.